


Prognostic Value of EEG Microstates in Acute Stroke

Filippo Zappasodi^{1,2}  · Pierpaolo Croce^{1,2} · Alessandro Giordani³ · Giovanni Assenza⁴ · Nadia M. Giannantoni^{5,6} · Paolo Profice⁵ · Giuseppe Granata⁵ · Paolo M. Rossini^{5,7} · Franca Tecchio⁶

Received: 26 October 2016 / Accepted: 17 May 2017 / Published online: 25 May 2017
© Springer Science+Business Media New York 2017

Abstract Given the importance of neuronal plasticity in recovery from a stroke and the huge variability of recovery abilities in patients, we investigated neuronal activity in the acute phase to enhance information about the prognosis of recovery in the stabilized phase. We investigated the microstates in 47 patients who suffered a first-ever mono-lesional ischemic stroke in the middle cerebral artery territory and in 20 healthy control volunteers. Electroencephalographic (EEG) activity at rest with eyes closed was acquired between 2 and 10 days (T0) after ischemic attack. Objective criteria allowed for the selection of an optimal number of microstates. Clinical condition was quantified by the National Institute of Health Stroke Scale (NIHSS) both in acute (T0) and stabilized (T1, 5.4 ± 1.7 months) phases and Effective Recovery (ER) was calculated as

$(\text{NIHSS}(T1) - \text{NIHSS}(T0)) / \text{NIHSS}(T0)$. The microstates A, B, C and D emerged as the most stable. In patients with a left lesion inducing a language impairment, microstate C topography differed from controls. Microstate D topography was different in patients with a right lesion inducing neglect symptoms. In patients, the C vs D microstate duration differed after both a left and a right lesion with respect to controls (C lower than D in left and D lower than C in right lesion). A preserved microstate B in acute phase correlated with a better effective recovery. A regression model indicated that the microstate B duration explained the 11% of ER variance. This first ever study of EEG microstates in acute stroke opens an interesting path to identify neuronal impairments with prognostic relevance, to develop enriched compensatory treatments to drive a better individual recovery.

✉ Filippo Zappasodi
f.zappasodi@unich.it

- ¹ Department of Neuroscience, Imaging and Clinical Sciences, “Gabriele d’Annunzio” University of Chieti-Pescara, via dei Vestini 31, 66100 Chieti, Italy
- ² Institute for Advanced Biomedical Technologies, “Gabriele d’Annunzio” University of Chieti-Pescara, Chieti, Italy
- ³ Medical Statistics and Information Technology, Fatebenefratelli Foundation for Health Research and Education, AFaR Division, Rome, Italy
- ⁴ Clinical Neurology, Campus Biomedico University of Rome, Rome, Italy
- ⁵ Department of Geriatrics, Neurosciences & Orthopaedics, Institute of Neurology, Catholic University of Sacred Heart, Policlinic A. Gemelli Foundation, Rome, Italy
- ⁶ Laboratory of Electrophysiology for Translational neuroscience (LET’S) – ISTR – CNR, at Department of Neuroscience, Fatebenefratelli Hospital, Rome, Italy
- ⁷ IRCCS S. Raffaele-Pisana, Rome, Italy

Keywords Microstates · Acute stroke · Prognosis · Resting state · Electroencephalography (EEG)

Introduction

Stroke is a leading cause of motor disability (Feigin et al. 2014; Crichton et al. 2016). Care in the hyper-acute and acute period after a stroke has improved over the past two decades, with a dramatic amelioration of stroke survival (<http://www.rcplondon.ac.uk/resources/stroke-guidelines>). It is a common experience that the outcome shows a huge inter-individual variability, even with similar symptoms and features of the lesion (site/volume) at onset (Zeiler and Krakauer 2013). Functional recovery typically takes place in the first 8–12 weeks after a stroke (Biernaskie et al. 2004), with a decremented progression in the following period, assessing to an asymptotic pattern (Duncan

et al. 1992). For this reason, an accurate identification of the neural markers of the neurological impairment in acute phase, as well as their prognostic value, could provide information about the selection of a therapy, medical and/or rehabilitative, that enhances the individual ability for post-acute recovery. Neural electric activity features *per se* hold a special usefulness in describing the functional state of neurons surviving cerebral ischemia after a stroke and in providing information about the outcome, especially if we consider that a neuro-vascular uncoupling occurs in stroke patients (Rossini et al. 2004). Indeed, Magnetoencephalographic (MEG) and Electroencephalographic (EEG) studies demonstrated that at rest and evoked cortical activities are highly sensitive to acute neurological impairment. Slow frequency power enhancement or alpha rhythm slowing are the most frequent findings in patients affected by acute stroke (Nuwer et al. 1987; Jerret and Corsak 1988; Niedermeyer 1997; Logar and Boswell 1991; Fernandez-Bouzas et al. 2000; Tecchio et al. 2005), correlating with both the clinical status (Finnigan et al. 2004; Assenza et al. 2009) and the lesion site (Murri et al. 1998). Somatosensory evoked cerebral activity proved to be highly reliable in monitoring cerebral ischemia effects (Beese et al. 1998; Oliviero et al. 2004; Moritz et al. 2007; Assenza et al. 2009). Moreover, evidence of neurophysiological indexes in acute phase predicting clinical outcome at six/nine months have been provided: low band (delta and theta frequency bands) increase associated with worst clinical recovery in stabilized phase (Cuspineda et al. 2003, 2007; Finnigan et al. 2004, 2007). When considering separately the activity of the two hemispheres, an enhancement of prognostic validity was observed, with the contralesional delta power increase adding a negative prognostic value to the clinical state in the acute phase (Tecchio et al. 2007; Zappasodi et al. 2007; Assenza et al. 2013).

Recently, the modular view of the brain as a dynamic hierarchical architecture of functional networks provides new insights into the understanding of the neurological deficits caused by a focal brain lesion. Going back about a century, the notion of ‘diaschisis’, introduced by Von Monakow (1914), refers to a sudden inhibition of function produced by an acute focal disturbance in a portion of the brain at a distance from the original site of injury, but anatomically connected with it through fibre tracts or functionally connected. Indeed a lesion, also if focal, disrupts the connectivity between the lesioned area and anatomical/functional connected regions, leading to the dysfunction of the whole network and manifesting through neurological symptoms which are more complex than those solely due to the damaged area alone (Corbetta 2012). Evidence has been provided that in acute and chronic stroke stages a network-based approach is

useful for understanding the link between neural activity dysfunctions and behavioural deficits (Grefkes and Fink 2011). Indeed, the interhemispheric interplay in preserving neurological function and sustaining recovery after an acquired brain lesion (Wu et al. 2011; Graziadio et al. 2012; Pellegrino et al. 2012), as well as the relationship between specific patterns of dysfunctions of Resting State Networks (RSNs) and specific behavioural deficits, have been evidenced both in functional Magnetic Resonance Imaging (fMRI) and EEG studies (Grefkes et al. 2008; Sharma et al. 2009; James et al. 2009; Carter et al. 2010; Wu et al. 2015; Baldassarre et al. 2016; Siegel et al. 2016).

Several previous studies demonstrated that the resting state EEG can be represented as a sequence of topographies that remain stable for about 40–120 ms, namely microstates (Fig. 1, Khanna et al. 2015). These topographies derive from the synchronous activities of neuronal ensembles and must have been generated by activity of different neuronal generators reflecting different functions (Lehmann et al. 1987, 1998). In this way, the microstate analysis allows assessing networking features of the brain via EEG, regardless of the choice of reference and without selecting a priori the models of the intra-cerebral electric currents (Lehmann and Skrandies 1980). That is, a microstate may be associated to a functional brain state during the occurrence of a specific neural process. Indeed, each microstate is characterized by a unique and fixed polarity-independent EEG spatial distribution, to which corresponds a fixed configuration of a distributed active neuronal network. Brain activity is thus globally modelled as a sequence of microstates (Koenig et al. 1999; Michel et al. 2001; Musso et al. 2010). Such a topographical approach can provide a more informative framework and global interpretability without any type of a priori hypothesis (Murray et al. 2008), in contrast with most of the EEG waveform analysis techniques, which aim at evaluating the brain’s electrical field in a specific location (for example by a priori choice of electrodes of interest) or at determinate time intervals or in specific frequency bands. In this framework, a general quoted hypothesis, that considers the brain activity in a modular point of view, is that the microstates are “the building blocks of thought” and information processing (Lehmann and Skrandies 1980, 1987). Microstate analysis can reveal the significance of modular aspects of brain dynamics and their role in behavioural control as well as in the characterization of brain diseases (Lehmann and Skrandies 1980, 1987, 1998; Koenig et al. 1999, 2002; Musso et al. 2010; Britz et al. 2010).

To our knowledge, no studies have been performed on the possible differences between neural activity of healthy

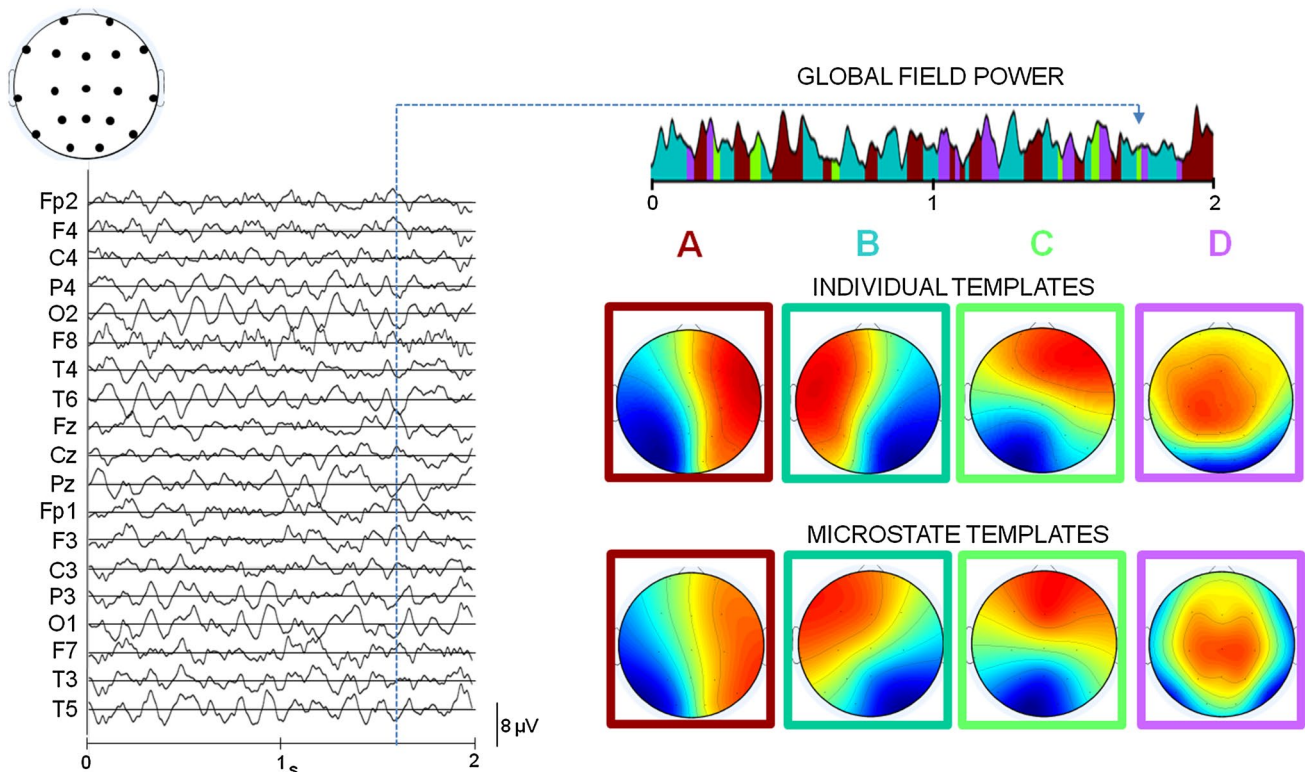


Fig. 1 For a representative healthy subject, a 2 s trial of EEG activity at rest with eyes closed is shown (data referenced to the common average, *Left bottom*) for each of the 19 EEG sensors (their location in *Left top*). The Global Field Power (GFP), a global measure of EEG amplitude, was computed for each time point (*Right top*) as standard deviation of the EEG signal across electrodes. Each colored area of GFP corresponds to an EEG topography which remains stable for that period, indicated with the corresponding color-code. We report the four topographies found for this subject (*Right middle*: named A, B, C and D). In each topographic map the color scale represents the

normalized value of electric potential on the scalp. The four maps of the single subject are similar to those obtained at group level (*Right bottom*). By the microstate analysis, the EEG time course of this subject is modeled as a sequence of the four ‘topographies’ also called templates or states or microstates. In this way, every time point from every subject is assigned to one of four templates. For each microstate the analysis calculates the following metrics: the duration of microstate, the number of times it occurred per second, the percentage of total time that is covered by the microstate

subjects and stroke patients on the basis of the spatio-temporal pattern of the EEG microstates. Indeed, if microstate brain transitions describe the fluctuations across main mode states of cerebral networks, then it is certainly expected that stroke patients will express a clear change of microstate characteristics. In particular, due to distorted cerebral connectivity after a stroke, we pose the working hypothesis that resting state microstates will differ in stroke patients with respect to healthy subjects. Such differences could represent an important electrophysiological marker for ischemic damage assessment, for outcome prediction and rehabilitation pathways selection. Here, we analysed the EEG data of stroke patients in acute phase at rest by means of the microstate analysis method. EEG microstate indices were compared between stroke patients and healthy controls and they were related to the clinical status in acute phase, as well as to the clinical outcome at 6 months.

Materials and Methods

Patients and Neurological Status Assessment in Acute Phase

Forty-seven patients (73.5 ± 8.8 years, 20 women and 27 men) suffering from a first-ever mono-hemispheric and mono-lesional ischemic stroke in the middle cerebral artery (MCA) territory were enrolled in the study. Patients were admitted to a network of clinical centres, allowing follow-up from acute stroke stage through the recovery process (1. S. Giovanni Calibita Hospital and 2. Fondazione Policlinico Agostino Gemelli in Rome; 3. San Raffaele Hospital, Cassino). The inclusion criteria were: clinical evidence of motor/sensory deficit of the upper limb; neuroradiological diagnosis of MCA ischemia. The exclusion criteria were: a previous stroke revealed by clinical history; neuroradiological evidence

of involvement of both hemispheres or brain haemorrhage; dementia or aphasia severe enough to impair patients' compliance with the procedures; anti-epileptic and anti-psychotic treatments. Patients received a diagnostic/therapeutic approach following the Italian stroke guidelines (SPREAD–Stroke Prevention and Educational Awareness Diffusion. Ictus cerebrale: Linee guida italiane; <http://www.spread.it>). Clinical status was quantified upon Stroke Unit arrival and between the 2nd and the 10th day after stroke onset (T0), by means of the National Health Institute Stroke Scale (NIHSS). Electroencephalogram (EEG) and Magnetic Resonance Imaging (MRI) were also collected at T0. Only patients with NIHSS scores greater than 2 were included in the study. NIHSS was repeated after 6 months (T1; 5.4 ± 1.7 months). For each patient, the same clinician assessed the NIHSS scores both at T0 and at T1. The effective recovery (ER) was then calculated as $ER = (NIHSS \text{ at } T0 - NIHSS \text{ at } T1) / NIHSS \text{ at } T0$. The NIHSS related to the upper limb was also obtained both at T0 and T1 and the effective recovery of upper limb was consequently calculated.

Patients with a lesion in the left hemisphere were also classified on the basis of presence or absence of language impairment and patients with a lesion in the right hemisphere were classified on the basis of presence or absence of spatial neglect.

Twenty healthy volunteers, matched for age and gender with patients, were also enrolled as the control group (mean age 71.5 ± 6.4 years, 7 females and 13 males, independent t-test for age between patients and controls: $p > 0.200$). All healthy subjects were not receiving any pharmacological treatment at the time of recordings and resulted normal at both neurological and brain magnetic resonance examinations.

Healthy subjects and patients were right-handed, as confirmed by the Edinburgh Manuality test (Oldfield 1971).

Five minutes of EEG activity was acquired at rest, while subjects sat on a comfortable armchair or laid on a hospital bed with their eyes closed. The EEG activity was recorded by 19 Ag-AgCl cup electrodes positioned according to the 1020 International EEG system (F1, F7, T3, T5, O1, F3, C3, P3, FZ, CZ, PZ, F2, F8, T4, T6, O2, F4, C4, P4) in fronto-central reference, an additional electrode pair served for recording electrooculogram to control for eye blinking. The impedances were kept below 5 k Ω . The Electrocardiogram was monitored by one bipolar channel placed on the chest. EEG data were sampled at 256 Hz (pre-sampling analogical filter 0.1–70 Hz), and collected for off line processing.

The experimental protocol was approved by the Hospital Ethical Committees, and all patients and healthy controls signed a written informed consent.

Data Analysis

Data were visually inspected to exclude saturated epochs of EEG signals from further analysis. A semi-automatic procedure, based on Independent Component Analysis (Barbati et al. 2004), was applied to identify and remove ocular, cardiac and muscular artifacts. Data were filtered between 1 and 30 Hz (Butterworth filter of 2nd order, forward and back filtering) and referenced to the common average. Epochs of 2 s were considered for microstate analysis (Fig. 1).

The procedure detailed in Murray et al. (2008) was followed to choose the optimal number of microstate templates. Briefly, for each subject separately, the maxima values of the Global Field Power (GFP) were extracted from the EEG time course. GFP is the standard deviation of the EEG signal across electrodes and represents a global measure of the EEG strength. Therefore, its peaks are periods of maximal power reflecting the highest topographic stability (Murray et al. 2008). The extracted GFP peaks were then submitted to a modified version of k-means clustering algorithm to identify the dominant topographies (Pascual-Marqui et al. 1995). We selected the number of EEG distribution templates between 1 and 10. The optimal number of templates was chosen for each subject based on the Cross-Validation (CV) criterion and Krzanowski-Lai (KL) criterion. Each criterion was calculated for each of the ten templates and, as suggested in Murray et al. (2008), the optimal number corresponded to the second maximum value of the KL and the minimum value of the CV. CV and KL agreed on the ideal number of microstates in 14/20 subjects (70%) in the group of healthy controls and in 35/47 subjects (74%) in the group of patients. In the cases of discordance, following the methods of others studies (Hatz et al. 2016; Gschwind et al. 2016), only the KL criterion was considered.

Mean templates of each group were computed re-clustering the subject-wise maps in the following way. Firstly, four random maps were selected from the subject-wise maps as initial templates. Then the four maps of each subject were assigned to each template on the basis of the best fit of the correlation between them. The new templates were obtained by averaging the maps assigned to each template. This procedure was repeated 30 times and the iteration with the lowest inter-subject variance was chosen. The four templates resulting from this procedure were paired between groups, by ensuring the minimal maps dissimilarity. According to Koenig and Melie-Garcia (2009), the generalized dissimilarity is defined as:

$$s = \sum_{i=1}^G \sqrt{\frac{\sum_{j=1}^N (\bar{v}_{ij} - \bar{v}_j)^2}{N}}$$

where \bar{G} is the number of groups, N is the number of electrodes, v_{ij} is the grand average across the subjects of the electric potential at electrode j for group i , and \bar{v}_j is the mean across groups of the electric potential at electrode j .

Considering the four templates of the control group, we observed topographies similar to those obtained in previous works (as for example in Koenig et al. 2002). So we labeled the microstates following the same order of literature (Fig. 1): A had a left occipital-parietal (negative) to right fronto-central (positive) orientation; B the opposite, right parieto-occipital to left fronto-central; C had a symmetrical back to prefrontal orientation; D a central positivity, with an occipital to fronto-central symmetrical orientation (see Koenig et al. 1999 for details).

To test for differences between the group mean templates, we first performed a permutation analysis using the generalized dissimilarity as a measure of the effect size. In particular, a distribution of the measures of the effect size was simulated under the null hypothesis by randomly mixing iteratively the subject templates and then by computing, at each iteration, the effect size. Then the statistical significance was calculated in refusing the null hypothesis by computing the times in which the effect size under the null hypothesis is greater than or equal to the actual effect size. With 5000 iterations, it is possible to assess a level of statistical significance equal to 1% (see Koenig and Melie-Garcia 2009 for details). Subsequently, only for those templates resulting above the statistical significance from the previous analysis, post-hoc tests were performed to assess the differences between specific groups. The post-hoc analysis was performed in the same way as the group analysis, by considering global dissimilarity as a measure of the effect size. The global dissimilarity, for two maps u and v , is defined as follows:

$$GD_{u,v} = \sqrt{\frac{1}{N} \sum_{i=1}^N \left(\frac{u_i}{GFP_u} - \frac{v_i}{GFP_v} \right)^2}$$

where u_i , v_i are the electric potentials of the i_{th} electrode for the maps u and v respectively, $GFP_{u,v}$ are the global field powers of the maps and N is the number of electrodes.

The obtained group-wise templates were then fitted backward to the original data to compute the metrics and the syntax of the microstates. The back-fitting procedure was based on the maximum correlation between each template and the topography at each time instant and was performed with the Cartool software (Brunet et al. 2011). Such a procedure allows us to represent the EEG time course in terms of microstates, i.e. potential distributions on the scalp, which occur frequently, and to extrapolate variables of interest. As required by the procedure, for

each subject and for each microstate class, the following metrics were calculated (Brunet et al. 2011):

1. Mean microstate duration: average time covered by a single microstate class.
2. Mean percentage of covered analysis time: percentage of time covered by a single microstate class.
3. Mean occurrences per second: mean number of distinct microstates of a given class occurring within a 1 s window.

Furthermore, the mean global explained variance was obtained as the sum of the explained variances weighted by the global field power taking into account all four microstates. This parameter expresses the quality of the fit of the microstate templates to the EEG data.

According to Brunet et al. (2011) we evaluated also microstate syntax, i.e. the probabilities of transition from one state (represented by a template) to another. Then the ‘directional predominance’ was evaluated (Lehmann et al. 2005) to quantify the directional asymmetries in the transitions between two microstates. Six possible microstate values were evaluated, corresponding to the six possible microstate pairs ($A \leftrightarrow B$, $A \leftrightarrow C$, $A \leftrightarrow D$, $B \leftrightarrow C$, $B \leftrightarrow D$, $C \leftrightarrow D$). A significant positive value of $X \leftrightarrow Y$ corresponds to a higher probability to transit from X to Y with respect to transit from Y to X , and the negative value corresponds to the opposite predominance to transit from Y to X .

Statistical Analysis

The differences of microstate metrics (microstate duration, occurrences per second, percentage of covered analysis time) among groups were evaluated by repeated-measures ANOVA, with *Group* (Healthy controls, Patients with lesion in the left hemisphere, Patients with lesion in the right hemisphere) as between-subject factor and *Template* and *Hemisphere* (Left, Right) as within subject factors. Greenhouse-Geisser correction has been applied when the sphericity assumption was not valid. When an interaction *Group X Template* was found, reduced ANOVA models were carried out separately for each template, with *Group* as between-subject factor. Significant main effect of *Group* for each template was followed up by post-hoc unpaired t-test, Bonferroni corrected, to compare microstate metrics among groups. The values of the healthy control group were considered as the reference.

To assess differences in directional predominance between patients and controls, for each transition probability an ANOVA design was applied, with *Pairs* ($A \leftrightarrow B$, $A \leftrightarrow C$, $A \leftrightarrow D$, $B \leftrightarrow C$, $B \leftrightarrow D$, $C \leftrightarrow D$) as within-subject factor and *Group* (Healthy controls, Patients with lesion in the left hemisphere, Patients with lesion in the right

hemisphere) and as between-subject factor. When an interaction *Group X Pairs* was found, reduced ANOVA models were carried out separately for each pair, with *Group* as between-subject factor.

Post-hoc comparison were performed to compare microstate directional predominance values of left and right patients with the values of the control group, used as the reference. Post-hoc comparisons were Bonferroni corrected.

A first exploratory correlation analysis between clinical scores and microstate characteristics was performed. Specifically, Spearman's correlations were carried out between clinical scores (NIHSS at T0 and NIHSS at T1 global and related to the upper limb) and both microstate metrics and directional predominance. Pearson's correlations between Effective Recovery (global and related to the upper limb) and both microstate metrics and directional predominance were also carried out.

Finally, to check for a possible relationship between microstate characteristics in acute phase and clinical recovery, the Effective Recovery scores were linearly regressed against microstate metrics and directional predominance. Clinical condition in acute phase also entered the model as an independent variable. Even if the sample size of the present study was larger than many other neurophysiological published papers, it did not allow us, strictly speaking, to reach a cases-per-variable ratio usually considered appropriate to provide stability to the prognostic models. For such a reason, we chose to reduce the number of potential predictors considering only those variables which showed a significant difference between stroke patients and controls and a significant correlation with the clinical status in acute or stabilized phase.

Results

Patients Findings

NIHSS score in the acute phase in patients ranged from 3 to 22 (median: 6.0; 5–95 percentile: 3–18). Stroke was localized in the left hemisphere in 30 patients (NIHSS range 3–22; median 6) and in the right hemisphere in the remaining 17 (NIHSS range 3–18, median 6.0).

According to the differences between NIHSS at T0 and NIHSS at T1 and to the ER values, all patients showed at least some clinical recovery at T1 (median of NIHSS: 2.0; 5–95 percentile: 0–11.4). In particular 8 patients (17% of all patients) showed a complete recovery (ER=1). Right-lesion and left-lesion patients did not differ either for NIHSS in acute phase (Mann Whitney test: $p=0.490$), or for NIHSS in stabilized phase ($p=0.884$) or for effective recovery ($p=0.885$).

73% of patients with lesion in the left hemisphere had language impairment. Only 3 patients with lesion in the right hemisphere had spatial neglect. Since this number was very low, no further statistical analysis was performed comparing the right lesioned patients having or not having spatial neglect.

Microstates

Applying the criteria for optimal number of templates, we identified three templates in 15 people (5 healthy controls, 4 patients with left lesion, 6 patients with right lesion), four templates in 49 people (14 healthy subjects, 24 patients with left lesion, 11 patients with right lesion) and five templates in 3 people (1 healthy control, 2 patients with left lesion). We did not find a difference in the prevalence of the number of templates across the two populations (three templates in 25% of healthy control=HC and 21% of patients=P; four templates in 70% HC and 75% P; five templates in 5% HC and 4% P). For this reason, we fixed the number of templates in each subject based on the 74% mean prevalence of the four templates (49 out of 67) to execute the comparison between patients and healthy controls.

The Global Explained Variance was not different across the healthy controls and patient groups ($72.1 \pm 6.2\%$ for controls; $74.3 \pm 6.1\%$ for patients with lesion in the left hemisphere; $73.9 \pm 6.8\%$ for patients with lesion in the right hemisphere; ANOVA design, factor *Group*: $p > 0.5$).

Studying the four templates across the three groups of control subjects, and the patients divided based on the lesion site, no differences were found between healthy templates and right hemispheric stroke patients' templates. The only alteration regarded the C map, which differed between healthy group and the group of patients with a lesion in the left hemisphere ($p < 0.001$, Fig. 2). The alteration of C map in patients with left lesion is driven by the patients with language impairment. Indeed, the mean map of template C of these patients looks different from the corresponding template of healthy controls ($p < 0.001$, Fig. 3). Also for patients with a right lesion, the mean map of template D of the 3 patients with spatial neglect was different from the template of healthy controls ($p < 0.001$, Fig. 3).

The repeated measures ANOVA with *Group* as between-subject factor and *Template* (A, B, C and D) as within subject factor showed different mean values of template metrics among groups, as evidenced by the significant interaction *Group X Template* ($p < 0.05$ consistently, Table 1). In particular, reduced models and post-hoc analyses showed microstate metrics dependent on the lesion side: (a) microstate duration, (b) frequency of occurrence per second, (c) percentage in coverage of template C were lower in left-lesioned with respect to the right-lesioned patients (Fig. 4), while all three metrics were higher in

Fig. 2 Group mean templates of microstates (A, B, C and D) obtained for healthy controls, patients with lesion in the *left* hemisphere, patients with lesion in the *right* hemispheres

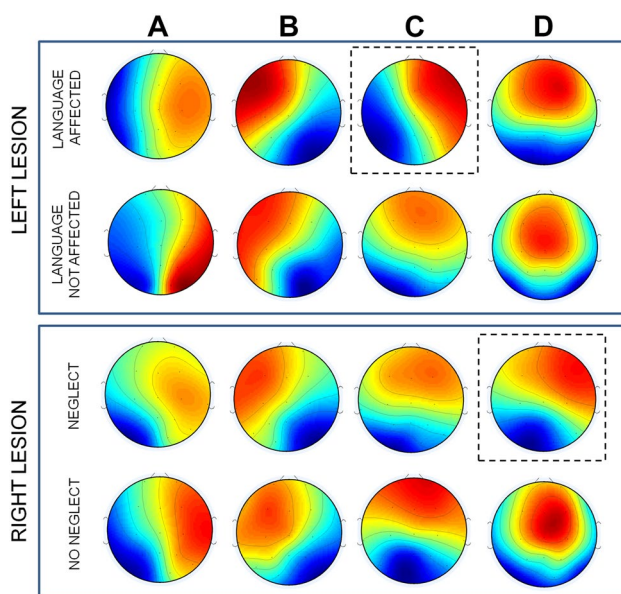
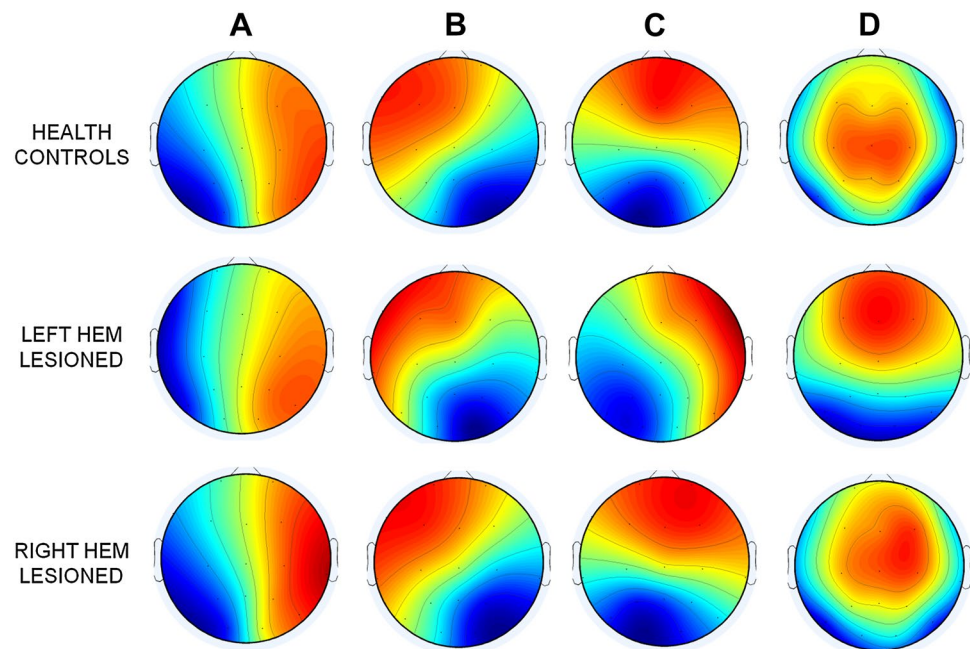


Fig. 3 Mean of the topography of microstates (A, B, C and D) obtained (1) for patients with lesion in the *left* hemisphere differentiated on the basis of the presence of language impairment (*top*); (2) for patients with lesion in the *right* hemisphere differentiated on the basis of the presence of neglect (*bottom*). Dotted boxes represent significant difference from the corresponding topography of healthy controls, assessed by TANOVA ($p < 0.001$)

left-lesioned with respect to right-lesioned patients for template D (Fig. 4). Given the opposite changes of microstate C and D in patients with respect to controls, we evaluated the ratio of template D over template C metrics and we compared them between patients and controls. Left patients

showed higher values of D vs C duration ratio than controls (1.11 ± 0.30 vs 0.90 ± 0.21 , independent t-test $p = 0.021$), while right patients had lower values (0.75 ± 0.22 vs 0.90 ± 0.21 , independent t-test $p = 0.041$).

No differences were found neither between all microstate metrics of left patients having and not having language impairment, nor between all microstate metrics of left patients with language impairments and healthy controls (consistently, independent t-test: $p > 0.200$).

The analysis of microstate directional predominance revealed a significant interaction *Pair X Group* ($p < 0.05$, Table 1). Reduced models performed separately for each pairs showed the significance of the Group factor for the B \leftrightarrow D and C \leftrightarrow D transactions. In particular, post-hoc comparisons showed that the directional predominance for B \leftrightarrow D and C \leftrightarrow D was lower in patients with the lesion in the right hemisphere with respect to patients with the lesion in the left hemisphere (Fig. 4). The one-tailed t-test of these values demonstrated that directional predominance was significantly less than zero (A \leftrightarrow D: $t(16) = -2.128$, $p = 0.049$; B \leftrightarrow D: $t(16) = -4.632$, $p < 0.001$; C \leftrightarrow D: $t(16) = -4.816$, $p < 0.001$), i.e. in patients with a right lesion the probability to enter in microstate D is smaller than the probability to depart from it (Fig. 4).

Relationship Between Microstate Metrics and Syntax and Clinical Assessment

The metrics of microstate B correlated with the Effective Recovery. Indeed, a longer duration and a higher percentage in coverage of the microstate B in acute phase

Table 1 Microstates dynamics

	Full model			Reduced model-single template/pair (df: 2,64)					
	df	F	p value	A	B	C	D		
Microstate duration									
Group	ns	ns	ns	ns	ns	5.410	8.386		
Template	3; 192	4.205	0.007			0.007	0.001		
Group*template	6; 192	4.133	0.001						
Frequency of occurrence per second									
Group	ns	ns	ns	ns	ns	4.345	3.503		
Template	2.5; 162.7	5.171	0.003			0.017	0.036		
Group*template	5.1; 162.7	2.345	0.043						
Percentage in coverage									
Group	ns	ns	ns	ns	ns	5.479	5.737		
Template	3; 192	4.736	0.003			0.006	0.005		
Group*template	6; 192	3.295	0.004						
Directional predominance				A↔B	A↔C	A↔D	B↔C	B↔D	C↔D
Group	ns	ns	ns	ns	ns	ns	ns	3.417	6.375
Pair	3; 192	4.992	0.002					0.039	0.003
Group*pair	6; 192	2.377	0.031						

Comparison between stroke patients and control subjects

Results of repeated measures ANOVA for each microstate metric and for directional predominance, with *Group* as between-subject factor and *Template* (A,B,C and D) or *Pair* (A ↔ B, A ↔ C, A ↔ D, B ↔ C, B ↔ D, C ↔ B) as within-subject factor. Whenever the significance of the interaction *Group*Template* or *Group*Pair* was found, we executed the ANOVA of the reduced model for each template (or each pair) separately, with *Group* as between-subject factor (Reduced Model-single Template)

ns p>0.05

correlated with a better recovery (Fig. 5, Pearson's correlation: $r=0.380$; $p=0.009$ and $r=0.326$, $p=0.027$; respectively). This relationship was found also for clinical scores of the upper limb (Pearson's correlation between upper limb recovery and microstate B duration: $r=0.359$, $p=0.034$; microstate B coverage: $r=0.368$, $p=0.030$). No correlations were found between microstate metrics and clinical status at T0. Conversely, in the stabilized phase, a slight positive correlation was present between duration of the microstate B and both global NIHSS (Spearman's $\rho = -0.356$, $p=0.016$) and upper limb score ($\rho = -0.347$, $p=0.035$). These correlations indicated a worse clinical status related to lower values of microstate B metrics.

No correlations were found between directional predominance and clinical status (both at T0 and at T1) and recovery.

Taking into account that patients and controls differed in microstate C and D metrics and that microstate B duration and coverage correlated with clinical status at T1, a regression analysis with ER as the dependent variable and microstate C and D metrics and B duration and coverage as independent variables was assessed. The value of NIHSS in acute phase was also included as an independent variable. Only NIHSS in acute phase and microstate B duration

entered the model (Fig. 5). The 42% of ER variance was explained by this model ($F(2,44)=16.105$, $p<0.001$), with in particular 36% accounted for by NIHSS and the adjunctive 6% by microstate B duration. The coefficients of the model show that better clinical status at T0 and higher duration of microstate B predict a better recovery (Fig. 5). Moreover, in prognostic perspective, we checked the regression model without clinical status in acute phase. Only microstate B duration entered the model, with the 11% of ER variance explained ($F(1,45)=5.696$, $p=0.021$).

Discussion

Our main finding is that the dynamics of acute phase EEG microstates in patients affected by mono-hemispheric stroke informs us about the recovery ability in the stabilized phase. Preservation of one state (microstate B) in acute phase correlated with better outcome. That is, the more microstate B is preserved in the acute phase (higher duration, occurrence, coverage), the better the functional recovery will be in the stabilized phase. Microstate B has been associated to visual area activity (Britz et al. 2010) and visual processing (Seitzman et al. 2017). Therefore,

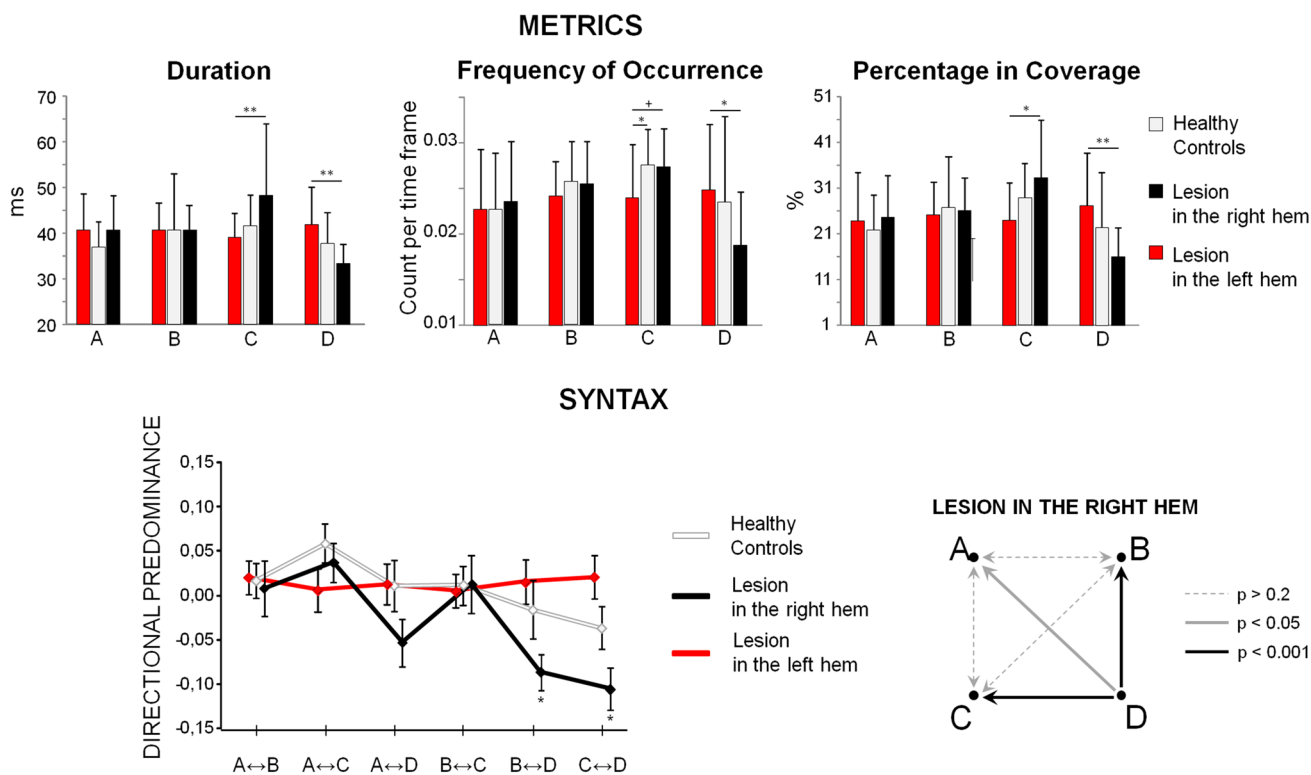


Fig. 4 *Top* Mean (standard deviation) of the microstate metrics for healthy controls (grey), patients with lesion in the left hemisphere (red), patients with lesion in the right hemisphere (black). Post-hoc comparison significances (Bonferroni corrected) are displayed: * $p < 0.050$. *Bottom* Mean (standard error) of the microstate directional predominance (left) for healthy controls (grey), patients with lesion in the left hemisphere (red), patients with lesion in the right hemisphere (black). Post-hoc comparison significances (Bonferroni corrected) are displayed: * $p < 0.050$. On the right, the directional

predominance of microstate concatenation for patients with lesion in the right hemisphere is displayed. The arrows indicate the significant direction of the transition (X to Y or Y to X), as established by the one sample t-test (difference from 0); bidirectional grey dotted line correspond to directional predominance values not different from 0 ($p > 0.200$), i.e. no directional predominance; grey ($p < 0.05$) and black ($p < 0.001$) lines evidence a predominance to transit from X to Y

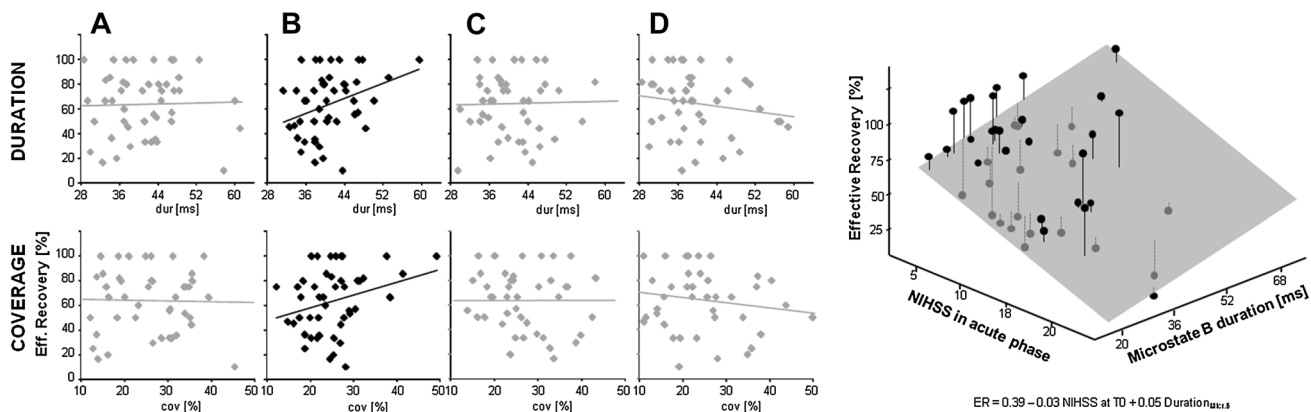


Fig. 5 *Left* Scatterplot of the Effective Recovery over duration and over coverage of microstates A, B, C and D. In the case of significant correlation the black color was used (otherwise the plot is grey). Regression lines are shown. *Right*: Scatterplot of Effective Recovery

over microstate B duration and NIHSS in acute phase. Regression plane is shown and the equation of the linear regression model is displayed

our results may underline the crucial role of the visual system and visuo-motor integration in driving plasticity phenomena to regain sensorimotor control. In healthy subjects, lack of visual feedback provoked a huge brain activation unrelated to the quality of execution in a simple handgrip. This evidence indicates the relevance of visuo-motor feedback even in online monitoring of everyday usual actions (Mayhew et al. 2017). In people with damaged proprioception, the feeling of controlling bodily movements is dominated by visual feedback (Evans et al. 2015). In stroke patients the visual feedback of the unaffected hand movement, rather than the motor output, drives the network interactions that sustain mirror feedback therapy in enhancing functional recovery (Saleh et al. 2017). Furthermore, the class B template is related to verbalization (Milz et al. 2016). In the light of this association, the current results could be interpreted as patients whose lesions do not affect language in acute phase have better outcomes. However, in our cohort, microstate B metrics were not different between patients having or not having language impairment and recovery was not related to the presence of language impairment, while this was the case for microstate C.

Since the dynamics of microstate fluctuations displays scale-free properties (Van De Ville et al. 2010), we can interpret our prognostic microstate result consistent with recent findings about the fractal dimension of the global EEG activity in the acute stroke patients. In particular, larger asymmetries of hemispheric fractal dimension in acute phase correlated with worse clinical recoveries in the stabilized phase (Zappasodi et al. 2014). Here microstate analysis provides direct access to prognostic information, probably because each microstate quantifies complex network balances, while EEG channel fractal dimension needs the comparison between the two hemispheric values to express functionally relevant balances.

When studying the EEG fractal dimension (Zappasodi et al. 2014), it decreased after the stroke as compared with healthy controls and in proportion with the clinical severity, mirroring the global system dysfunction resulting from the structural damage. Conceivably, the decrease of the fractal dimension of the global EEG activity reveals the intimate nature of structure–function unity, where an anatomical lesion –even local and discrete– impairs the whole brain multi-scale self-similar activity. Here we observed that EEG microstate duration is informative about recovery, but not of the severity of the clinical state in acute phase. Conceivably, the wide state of networks mirrored in one microstate reveals more the long-range functional balances of networks than the current effect of single network damage. Consistently with this interpretation, from fractal dimension analysis we observed that only the interhemispheric unbalance, and not the overall values, informed us about recovery.

Consistently with this concept, EEG studies investigating the prognostic value of acute phase neuronal activity, found that the contralesional EEG delta activity, which retained relevant negative prognostic information, was an expression of a reduction of interhemispheric functional coupling. In other words, the maintenance of interhemispheric interplay is a decisive element for clinical recovery (Wu et al. 2011; Graziadio et al. 2012; Pellegrino et al. 2012) and a single microstate seems to reflect such a balance.

Here, according to the literature, we determined microstate features considering the neuronal activity in the frequency range between 1 and 30 Hz. Recently, the network features in acute stroke were assessed by graph theory and displayed network rearrangements mainly in delta, theta, and alpha bands (Caliandro et al. 2016). Future investigation will evaluate microstate features differentiating the frequency bands of the oscillatory EEG activity.

Definitely, the acute phase of stroke alters microstate dynamics. We evaluated for the first time EEG microstates at rest in patients affected by mono-hemispheric stroke in acute phase. Applying proper selection criteria, the four templates, namely A, B, C and D, typical of healthy controls (Lehmann et al. 1998; Koenig et al. 1999; Khanna et al. 2015), prevailed across the three groups of healthy subjects and patients depending on the damaged hemisphere. This is well consistent with literature, where the same four head-surface brain electric potential configurations optimally explained the variance of EEG distribution dynamics in resting state (Wackermann et al. 1993; Koenig et al. 2002; Milz et al. 2016).

The metrics derived from microstate dynamics have a slightly different neurophysiologic significance. The mean duration, named in several studies average lifespan, is interpreted to reflect the stability of its underlying neural assemblies. The frequency of occurrence of a particular microstate may reflect the tendency of its underlying neural generator to become activated. Finally, coverage quantifies the percentage of total time in which the microstate is dominant. It can be interpreted to reflect the amount of dominance of the underlying neural generators (Lehmann et al. 1987). Therefore, a reduction of the microstate metrics can be thought as disengagement and instability of the neural activity of the network generating the microstate topography and conversely an increase may be a sign of dysfunctional hyper-activity.

In stroke patients, consistently microstates C and D displayed opposite behaviors, with C less represented in left-damage, D less represented in right-damage, with healthy control inbetween. This opposite behavior of two states suggests that the balances of the dynamical interplay among microstates is more functionally relevant than the specific alteration of a single one.

The correspondence between a single microstate and a set of activated cerebral areas, as revealed by fMRI, or with a specific resting state network, or an ensemble of them, is not univocal in the literature. What is clear is that different microstates and corresponding topographies mirror distinct neuronal synchronized networks. Therefore, microstate dynamics reflects the dynamic synchronization of such functional network subunits. Interestingly, our investigation showed that microstate sequences clearly depended on the integrity of the cerebral structure, with the balance of states C and D displaying opposite occurrences depending on the damaged hemispheres. In fact, all microstate C metrics varied in the same direction, consistently showing shorter period of appearance, smaller frequencies of occurrence and smaller percentage of coverage in left damage than in right damage, while microstate D behaved in the opposite direction in this group of patients. Conversely, in the right patients the metrics of the microstate D were lower and those of microstate C higher. Interestingly, Seitzman et al. (2017), manipulating the eyes closed and eyes open condition with a cognitive task, found that the changes induced by the task to microstate C and D were in opposite direction from one another.

Template C is mainly associated to insula-cingulate salience network (Britz et al. 2010). In our data, the alteration of template C topography seen in the left patients was probably driven by the patients with language impairment. Indeed, Brownsett et al. (2014) underlined that tests probing language impairment in patients are dependent on domain-general processes. It can be hypothesized that the microstate associated with the salience network, in particular the dorsal anterior cingulate cortex and the nearby midline frontal cortex, is related to language-specific processing because of its association with domain-general, task-dependent processes.

Template D is less represented after a right lesion. Moreover, only for these patients the probability to transit to D from another microstate is reduced. Template D is mainly associated with focal attention network (Brandeis and Lehmann 1986; Britz et al. 2010) and its alteration may be present in patients with neglect syndrome. Future studies with a higher number of patients will investigate this hypothesis. Crucially, microstate occurrence unbalances with opposite alterations of C vs D and D vs C microstates as a consequence of both a left or right damage, underline the relevance of network activity balances for brain functionality. In particular, the equilibrium between focal attention and executive functions is mandatory for the brain functionality.

Our new finding integrates and extends knowledge about the crucial relevance of balances between homologous cerebral regions of the two hemispheres (Traversa et al. 1997; Oliveri et al. 1999, 2000; Wu et al. 2011; Pellegrino et al.

2012) and body sides (Graziadio et al. 2012), with the new evidence that brain functionality also requires a balance among occurrences of physiological fluctuations across different synchronized networks. Moreover, we found signs of the relationship between microstate alterations and clinical effects, with the alteration of specific topographies of microstates in aphasia and neglect. We can argue that the analysis of microstates—by catching synchronized macro-networks occurrences—enables the assessment of the functionally relevant networking of brain processing.

An attempt to find an association between the injury site and alteration of microstates and the metrics associated with them is beyond the scope of this work. To do this, further fMRI/EEG studies should be done in patients, with careful classification and diversity of lesion location. In particular, an accurate analysis of brain sources associated with each microstate should be done in patients, analysis possible only by means of the high-density EEG. Nevertheless, our results support the hypothesis that a finely tuned interplay between the main four EEG microstate classes is necessary to sustain brain functioning. Definitely, our data support the notion that a focal lesion drives a global malfunctioning of metrics and dynamics of microstates, with an excessive staying in some states with respect to others in a manner dependent on the lesion side.

In conclusion, our first ever study of microstates in acute stroke in relationship with recovery ability interestingly revealed that the dynamics of specific microstates inform us about the individual patient's prognosis. The importance of acute state prognostic factors to guide the selection of personalized rehabilitation treatments indicates the need to further develop this approach, which also estimates quantitatively the dynamics of the fluctuations of wide-range synchronized neuronal networks.

Acknowledgements The research leading to these results has received funding from: (1) The Italian Ministry of Health, Cod. GR-2008-1138642; (2) PNR-CNR Aging Program 2012–2018; (3) FISM – Fondazione Italiana Sclerosi Multipla –Prot. N. 13/15/F14. The authors want to acknowledge Peter Angelo Taliaferro for language editing.

References

- Assenza G, Zappasodi F, Squitti R, Altamura C, Ventriglia M, Ercolani M, Quattrocchi CC, Lupoi D, Passarelli F, Vernieri F, Rossini PM, Tecchio F (2009) Neuronal functionality assessed by magnetoencephalography is related to oxidative stress system in acute ischemic stroke. *NeuroImage* 44:1267–1273
- Assenza G, Zappasodi F, Pasqualetti P, Vernieri F, Tecchio F (2013) A contralesional EEG power increase mediated by interhemispheric disconnection provides negative prognosis in acute stroke. *Restor Neurol Neurosci* 31:177–188
- Baldassarre A, Ramsey L, Rengachary J, Zinn K, Siegel JS, Metcalf NV, Strube MJ, Snyder AZ, Corbetta M, Shulman GL.

- Dissociated functional connectivity profiles for motor and attention deficits in acute right-hemisphere stroke. *Brain* 139:2024–2038. doi:[10.1093/brain/aww107](https://doi.org/10.1093/brain/aww107)
- Barbati G, Porcaro C, Zappasodi F, Rossini PM, Tecchio F (2004) Optimization of ICA approach for artifact identification and removal in MEG signals. *Clin Neurophys* 115: 1220–1232
- Beese U, Langer H, Lang W, Dinkel M (1998) Comparison of near-infrared spectroscopy and somatosensory evoked potentials for the detection of cerebral ischemia during carotid endarterectomy. *Stroke* 29:2032–2037
- Biernaskie J, Chernenko G, Corbett D (2004) Efficacy of rehabilitative experience declines with time after focal ischemic brain injury. *J Neurosci* 24:1245–1254
- Brandeis D, Lehmann D (1986) Event-related potentials of the brain and cognitive processes: approaches and applications. *Neuropsychologia* 24:151–168
- Britz J, Van De Ville D, Michel CM (2010) BOLD correlates of EEG topography reveal rapid resting-state network dynamics. *Neuroimage* 52:1162–1170. doi:[10.1016/j.neuroimage.2010.02.052](https://doi.org/10.1016/j.neuroimage.2010.02.052)
- Brownsett SLE, Warren JE, Geranmayeh F, Woodhead Z, Leech R, Wise RJS (2014) Cognitive control and its impact on recovery from aphasic stroke. *Brain* 137:242–254
- Brunet D, Murray MM, Michel CM (2011) Spatiotemporal analysis of multichannel EEG: CARTOOL. *Comput Intell Neurosci* 2011:813870. doi:[10.1155/2011/813870](https://doi.org/10.1155/2011/813870)
- Caliandro P, Vecchio F, Miraglia F, Reale G, Della Marca G, La Torre G, Lacidogna G, Iacovelli C, Padua L, Bramanti P, Rossini PM (2016) Small-world characteristics of cortical connectivity changes in acute stroke. *Neurorehabil Neural Repair* 31:81–94
- Carter AR, Astafiev SV, Lang CE, Connor LT, Rengachary J, Strube MJ, Pope DL, Shulman GL, Corbetta M (2010) Resting inter-hemispheric functional magnetic resonance imaging connectivity predicts performance after stroke. *Ann Neurol* 67:365–375
- Corbetta M (2012) Functional connectivity and neurological recovery. *Dev Psychobiol* 54: 239–253
- Crichton SL, Bray BD, McKeivitt C, Rudd AG, Wolfe CDA (2016) Patient outcomes up to 15 years after stroke: survival, disability, quality of life, cognition and mental health. *J Neurol Neurosurg Psychiatry* 87:1091–1098
- Cuspidada E, Machado C, Aubert E, Galan L, Llopis F, Avila Y (2003) Predicting outcome in acute stroke: a comparison between QEEG and the Canadian Neurological Scale. *Clin Electroencephalogr* 34:1–4
- Cuspidada E, Machado C, Galan L, Aubert E, Alvarez MA, Llopis F, Portela L, Garcia M, Manero JM, Avila Y (2007) QEEG prognostic value in acute stroke. *Clin EEG Neurosci* 38:155–160
- Duncan PW, Goldstein LB, Matchar D, Divine GW, Feussner J (1992) Measurement of motor recovery after stroke. Outcome assessment and sample size requirements. *Stroke* 23:1084–1089
- Evans N, Gale S, Schurger A, Blanke O (2015) Visual feedback dominates the sense of agency for brain-machine actions. *PLoS ONE* 10:e0130019
- Feigin VL et al (2014) Global and regional burden of stroke during 1990–2010: findings from the global burden of disease study 2010. *Lancet* 383:245–254
- Fernandez-Bouzas A, Harmony T, Fernandez T, Silva-Pereyra J, Valdés P, Bosch J, Aubert E, Casián G, Otero Ojeda G, Ricardo J, Hernández-Ballesteros A, Santiago E (2000) Sources of abnormal EEG activity in brain infarctions. *Clin Electroencephalogr* 31:165–169
- Finnigan SP, Rose SE, Walsh M, Griffin M, Janke AL, McMahon KL, Gillies R, Strudwick MW, Pettigrew CM, Semple J, Brown J, Brown P, Chalk JB (2004) Correlation of quantitative EEG in acute ischemic stroke with 30-day NIHSS score. Comparison with diffusion and perfusion MRI. *Stroke* 35:899–903
- Finnigan SP, Walsh M, Rose SE, Chalk JB (2007) Quantitative EEG indices of sub-acute ischaemic stroke correlate with clinical outcomes. *Clin Neurophysiol* 118:2525–2532
- Graziadio S, Tomasevic L, Assenza G, Tecchio F, Eyre JA (2012) The myth of the ‘unaffected’ side after unilateral stroke: Is reorganization of the non-infarcted corticospinal system to re-establish balance the price for recovery? *Exp Neurol* 238:168–175
- Grefkes C, Fink GR (2011) Reorganization of cerebral networks after stroke: new insights from neuroimaging with connectivity approaches. *Brain* 134:1264–1276
- Grefkes C, Novak DA, Eickhoff SB, Dafotakis M, Küst J, Karbe H, Fink GR (2008) Cortical connectivity after subcortical stroke assessed with functional magnetic resonance imaging. *Ann Neurol* 63:236–246
- Gschwind M, Hardmeier M, Van De Ville D, Tomescu M I, Penner I K, Negelin Y, Fuhr P, Michel C M, Seeck M (2016) Fluctuations of spontaneous EEG topographies predict disease state in relapsing-remitting multiple sclerosis. *NeuroImage* 12:466–477
- Hatz F, Hardmeier M, Bousleiman H, Rüegg S, Schindler C, Fuhr P (2016) Reliability of functional connectivity of EEG applying microstates-segmented versus classical calculation of phase lag index. *Brain Connect* 6:461–469
- James GA, Lu ZL, VanMeter JW, Sathian K, Hu XP, Butler AJ (2009) Changes in resting state effective connectivity in the motor network following rehabilitation of upper extremity poststroke paresis. *Top Stroke Rehabil* 16:270–281
- Jerret SA, Corsak J (1988) Clinical utility of topographic EEG brain mapping. *Clin Electroencephalogr* 19:134–143
- Khanna A, Pascual-Leone A, Michel CM, Farzan F (2015) Microstates in resting-state EEG: current status and future directions. *Neurosci Biobehav Rev* 49:105–113. doi:[10.1016/j.neubiorev.2014.12.010](https://doi.org/10.1016/j.neubiorev.2014.12.010)
- Koenig T, Melie-Garcia L (2009) Statistical analysis of multichannel scalp field data. In: Michel CM, Koenig T, Brandeis D, Gianotti LRR, Wackermann J (eds) *Electrical neuroimaging*. Medicine, Cambridge, pp 169–180
- Koenig T, Lehmann D, Merlo MC, Kochi K, Hell D, Koukkou M (1999) A deviant EEG brain microstate in acute, neuroleptic-naïve schizophrenics at rest. *Eur Arch Psychiatry Clin Neurosci* 249:205–211
- Koenig T, Prichep L, Lehman D, Valdes Sosa P, Braeker E, Kleinlogel H, Isenhardt R, John ER (2002) Millisecond by millisecond, year by year: normative EEG microstates and developmental stages. *NeuroImage* 16:41–48.
- Lehmann D, Skrandies W (1980) Reference-free identification of components of checkboard-evoked multichannel potential field. *Electroencephalogr Clin Neurophysiol* 48:609–621
- Lehmann D, Ozaki H, Pal I (1987) EEG alpha map series: brain micro-states by space-oriented adaptive segmentation. *Electroencephalogr Clin Neurophysiol* 67:271–288
- Lehmann D, Strik WK, Henggeler B, Koenig T, Koukkou M (1998) Brain electric microstates and momentary conscious mind states as building blocks of spontaneous thinking: I. Visual imagery and abstract thoughts. *Int J Psychophysiol* 29:1–11
- Lehmann D, Faber PL, Galderisi S, Mucci A (2005) EEG microstate duration and syntax in acute, medication-naïve, first-episode schizophrenia: a multi-center study. *Psychiatry Res* 138:141–156
- Logar C, Boswell M (1991) The value of EEG mapping in focal cerebral lesions. *Brain Topogr* 3:441–446
- Mayhew SD, Porcaro C, Tecchio F, Bagshaw AP (2017) fMRI characterization of widespread brain networks relevant for behavioural variability in fine hand control with and without visual feedback. *Neuroimage* 148:330–342
- Michel CM, Thut G, Morand S, Khateb A, Pegna AJ, Peralta RG, Gonzales S, Seeck M, Landis T (2001) Electric source imaging of human brain functions. *Brain Res Rev* 36:108–118

- Milz P, Faber PL, Lehmann D, Koenig T, Kochi K, Pascual-Marqui RD (2016) The functional significance of EEG microstates-Associations with modalities of thinking. *Neuroimage* 125:643–656
- Moritz S, Kasprzak P, Arlt M, Taeger K, Metz C (2007) Accuracy of cerebral monitoring in detecting cerebral ischemia during carotid endarterectomy: a comparison of transcranial Doppler sonography, near-infrared spectroscopy, stump pressure, and somatosensory evoked potentials. *Anesthesiology* 107:563–569
- Murray MM, Brunet D, Michel CM (2008) Topographic ERP analyses: a step-by-step tutorial review. *Brain Topogr* 20:249–264. doi:10.1007/s10548-008-0054-5
- Murri L, Gori S, Massetani R, Bonanni E, Marcella F, Milani S (1998) Evaluation of acute ischemic stroke using quantitative EEG: a comparison with conventional EEG and CT scan. *Neurophysiol Clin* 28:249–257
- Musso F, Brinkmeyer J, Mobascher A, Warbrick T, Winterer G (2010) Spontaneous brain activity and EEG microstates. A novel EEG/fMRI analysis approach to explore resting-state networks. *Neuroimage* 52:1149–1161. doi:10.1016/j.neuroimage.2010.01.093
- Niedermeyer E (1997) Cerebrovascular disorders and EEG. In: Niedermeyer E, Lopes Da Silva F. (eds), *Electroencephalography: basic principles, clinical applications and related fields*, 4th edn., Williams & Wilkins, Baltimore, pp 320–321
- Nuwer MR, Jordan SE, Ahn SS (1987) Evaluation of stroke using EEG frequency analysis and topographic mapping. *Neurology* 37:1153–1159
- Oldfield RC (1971) The assessment and analysis of handedness: the Edinburgh inventory. *Neuropsychologia* 9:97–113
- Oliveri M, Rossini PM, Traversa R, Cicinelli P, Filippi MM, Pasqualetti P, Tomaiuolo F, Caltagirone C (1999) Left frontal transcranial magnetic stimulation reduces contralesional extinction in patients with unilateral right brain damage. *Brain* 122:1731–1739
- Oliveri M, Rossini PM, Filippi MM, Traversa R, Cicinelli P, Palmieri MG, Pasqualetti P, Caltagirone C (2000) Time-dependent activation of parieto-frontal networks for directing attention to tactile space. A study with paired transcranial magnetic stimulation pulses in right-brain-damaged patients with extinction. *Brain* 123:1939–1947
- Oliviero A, Tecchio F, Zappasodi F, Pasqualetti P, Salustri C, Lupoi D, Ercolani M, Romani GL, Rossini PM (2004) Brain sensorimotor hand area functionality in acute stroke: insights from magnetoencephalography. *NeuroImage* 23: 542–550.
- Pascual-Marqui RD, Michel CM, Lehmann D (1995) Segmentation of brain electrical activity into microstates: model estimation and validation. *IEEE Trans Biomed Eng* 42:658–665
- Pellegrino G, Tomasevic L, Tombini M, Assenza G, Bravi M, Sterzi S, Giacobbe V, Zollo L, Guglielmelli E, Cavallo G, Vernieri F, Tecchio F (2012) Inter-hemispheric coupling changes associate with motor improvements after robotic stroke Rehabilitation. *Restor Neurol Neurosci* 30:497–510
- Rossini PM, Altamura C, Ferretti A, Vernieri F, Zappasodi F, Caulo M, Pizzella V, Del Gratta C, Romani GL, Tecchio F (2004) Does cerebrovascular disease affect the coupling between neuronal activity and local haemodynamics? *Brain* 127:99–110
- Saleh S, Yarossi M, Manuweera T, Adamovich S, Tunik E (2017) Network interactions underlying mirror feedback in stroke: A dynamic causal modeling study. *NeuroImage* 13 46–54
- Seitzman BA, Abell M, Bartley SC, Erickson MA, Bolbecker AR, Hetrick WP (2017) Cognitive manipulation of brain electric microstates. *Neuroimage* 146:533–543. doi:10.1016/j.neuroimage.2016.10.002
- Sharma N, Baron J-C, Rowe JB (2009) Motor imagery after stroke: relating outcome to motor network connectivity. *Ann Neurol* 66:604–616
- Siegel JS, Ramsey LE, Snyder AZ, Metcalf NV, Chacko RV, Weinberger K, Baldassarre A, Hacker CD, Shulman GL, Corbetta M (2016) Disruptions of network connectivity predict impairment in multiple behavioral domains after stroke. *Proc Natl Acad Sci USA* 113:E4367–E4376. doi:10.1073/pnas.1521083113
- Tecchio F, Zappasodi F, Pasqualetti P, Tombini M, Salustri C, Oliviero A, Pizzella V, Vernieri F, Rossini PM, (2005) Rhythmic brain activity at rest from rolandic areas in acute mono-hemispheric stroke: a magnetoencephalographic study. *NeuroImage* 28: 72–83.
- Tecchio F, Pasqualetti P, Zappasodi F, Tombini M, Lupoi D, Vernieri F, Rossini PM (2007) Outcome prediction in acute mono-hemispheric stroke via magnetoencephalography. *J Neurol* 254:296–305
- Traversa R, Cicinelli P, Bassi A, Rossini PM, Bernardi G (1997) Mapping of motor cortical reorganization after stroke. A brain stimulation study with focal magnetic pulses. *Stroke* 28:110–117
- Van De Ville D, Britz J, Michel CM (2010) EEG microstate sequences in healthy humans at rest reveal scale-free dynamics. *Proc Natl Acad Sci USA* 107:18179
- Von Monakow C (1914) Die Lokalisation im Grosshirn und Abbau der Funktion durch kortikale Herde - Localization in the cortex and the reduction of cortical function. JF Bergmann (ed.) Wiesbaden
- Wackermann J, Lehmann D, Michel C, Strik W (1993) Adaptive segmentation of spontaneous EEG map series into spatially defined microstates. *Int J Psychophysiol* 14:269–283
- Wu W, Sun J, Jin Z, Guo X, Qiu Y, Zhu Y, Tong S (2011) Impaired neuronal synchrony after focal ischemic stroke in elderly patients. *Clin Neurophysiol* 122:21–26
- Wu J, Quinlan EB, Dodakian L, McKenzie A, Kathuria N, Zhou RJ, Augsburg R, See J, Le VH, Srinivasan R, Cramer SC (2015) Connectivity measures are robust biomarkers of cortical function and plasticity after stroke. *Brain* 138:2359–2369. doi:10.1093/brain/awv156
- Zappasodi F, Tombini M, Milazzo D, Rossini PM, Tecchio F (2007) Delta dipole density and strength in acute monohemispheric stroke. *Neurosci Lett* 416:310–314
- Zappasodi F, Olejarczyk E, Marzetti L, Assenza G, Pizzella V, Tecchio F (2014) Fractal dimension of EEG activity senses neuronal impairment in acute stroke. *Plos ONE* 9:e100199
- Zeiler SR, Krakauer JW (2013) The interaction between training and plasticity in the poststroke brain. *Curr Opin Neurol* 26:609–616